Recruitment of monocytes/macrophages by tissue factor-mediated coagulation is essential for metastatic cell survival and premetastatic niche establishment in mice

Ana M. Gil-Bernabé,[1] Špela Ferjančič,[1] Monika Tlalka,[1] Lei Zhao,[1] Philip D. Allen,[1] Jae Hong Im,[1] Karla Watson,[1] Sally A. Hill,[1] Ali Amirkhosravi,[2] John L. Francis,[2] Jeffrey W. Pollard,[3] Wolfram Ruf,[4] and Ruth J. Muschel[1]

[1]Gray Institute for Radiation Oncology and Biology, Department of Oncology, University of Oxford, Oxford, United Kingdom; [2]Center for Thrombosis Research, Florida Hospital, Orlando, FL; [3]Department of Developmental and Molecular Biology, Center for the Study of Reproductive Biology and Women's Health, Albert Einstein College of Medicine, New York, NY; and [4]Department of Immunology and Microbial Science, The Scripps Research Institute, La Jolla, CA

Tissue factor (TF) expression by tumor cells correlates with metastasis clinically and supports metastasis in experimental settings. However, the precise pathways coupling TF to malignancy remain incompletely defined. Here, we show that clot formation by TF indirectly enhances tumor cell survival after arrest in the lung, during experimental lung metastasis, by recruiting macrophages characterized by CD11b, CD68, F4/80, and CX$_3$CR1 (but not CD11c) expression. Genetic or pharmacologic inhibition of coagulation, by either induction of TF pathway inhibitor expression or by treatment with hirudin, respectively, abrogated macrophage recruitment and tumor cell survival. Furthermore, impairment of macrophage function, in either Mac1-deficient mice or in CD11b-diphtheria toxin receptor mice in which CD11b-positive cells were ablated, decreased tumor cell survival without altering clot formation, demonstrating that the recruitment of functional macrophages was essential for tumor cell survival. This effect was independent of NK cells. Moreover, a similar population of macrophages was also recruited to the lung during the formation of a premetastatic niche. Anticoagulation inhibited their accumulation and prevented the enhanced metastasis associated with the formation of the niche. Our study, for the first time, links TF induced coagulation to macrophage recruitment in the metastatic process. (*Blood*. 2012;119(13): 3164-3175)

Introduction

Clinical and experimental studies over the past 30 years have established that the coagulation system actively supports tumor progression and metastasis. Consistent with these observations, expression of procoagulants by tumor cells, among them tissue factor (TF), cancer procoagulant,[1] and selectin ligands, correlates with advanced disease and poor outcome for multiple cancer types.[2,3] TF (also known as coagulation factor III or CD142) is the protease receptor that initiates coagulation after injury through the extrinsic pathway. Under normal physiologic conditions, TF expression is limited to extravascular sites that only become exposed to blood after trauma. In this case, the exposed TF binds to and activates the blood-borne coagulation factor FVII, triggering clot formation through a cascade of proteolytic events that results in thrombin formation, activation of platelets, and fibrin deposition.[4]

In addition to triggering coagulation, the binding of FVIIa to TF activates intracellular signaling pathways through the TF cytoplasmic domain, by activating G-protein-coupled protease activated receptors (PARs), especially PAR2.[4] These signaling pathways support tumor angiogenesis[5,6] and regulate tumor progression.[7] Intracellular signaling pathways can be distinguished experimentally from the extracellular coagulative roles of TF by specific antibodies[7] or deletion of the cytoplasmic domain that eliminates many forms of TF signaling but still triggers coagulation.[6,8,9]

TF enhances tumor growth and angiogenesis,[4-7,10] and specifically plays an important role in some experimental models of hematogenous metastasis. In mice, inhibition of TF reduces metastasis. Conversely, TF expression by tumor cells may result in increased metastatic potential.[11-17] Indeed, metastatic cancer cells can express as much as 1000-fold higher levels of TF than their corresponding nonmetastatic cancer cells,[14] and cancer stem cells may also express higher levels of TF.[18] In some experimental settings, the cytoplasmic domain of TF has been proven to be required for maximal metastatic potential,[12,15,17,19] whereas in others it was dispensable.[20]

Thrombin activation is a critical common step in the coagulation cascade and an important determinant of metastasis.[21] The metastatic potential of tumor cells in murine models can be decreased by direct[22,23] or indirect inhibition of thrombin, based on a wide variety of pharmacologic or genetic means: deficiency in prothrombin or in fibrinogen, impairment of platelets, genetic deletion of the murine platelet thrombin receptor PAR4, and regulation of thrombin by endothelial thrombomodulin.[24] Taken together, these findings suggest that the TF-related metastatic potential is mainly directed through downstream thrombin generation and thrombin-mediated proteolysis,[1,3] and that activation of thrombin through other means would also stimulate metastatic potential.

Several mechanisms by which platelets, thrombin, and fibrin could help to support metastasis have been identified.[3] Among them are: tumor cell spreading,[25] protection from the intravascular shear forces, protection from NK cell killing and evasion of the immune system,[20,26,27] secretion of chemokines and cytokines that

may promote tumor cell migration, and proliferation and activation of the endothelium, promoting adhesion.[28] Recently, platelets have been shown to induce epithelial-mesenchymal-like transition in tumor cells, enhancing their metastatic potential, via TGF-β/Smad and NFκB pathways.[29] Here, we identify a previously unknown thrombin-dependent but NK-independent mechanism, in which TF-induced platelet clots recruit macrophages that are essential for in vivo tumor cell survival. Moreover, we uncover a crucial role for coagulation in the establishment of the premetastatic niche.

Methods

Cell culture, immunoblotting, and cell staining

The human A7, A7/TF, and A7/TFΔCD and the murine B16F10, B16F10-TF pathway inhibitor (TFPI), and B16F10-vector (pcDNA3.1/Zeo) melanoma cell lines have been previously described.[8,11] Details regarding cell culture and lysis can be found in supplemental Methods (available on the *Blood* Web site; see the Supplemental Materials link at the top of the online article).

Western blots were performed with the following antibodies: murine anti–human-TF-extracellular domain monoclonal antibody (TF9-10H10; Calbiochem), rabbit anti–human-TF-cytoplasmic domain polyclonal antibody (TFcT, generated in the laboratory of W.R.), and goat anti–mouse-TF polyclonal antibody (R&D Systems).

Cells were stained with 5-chloromethylfluorescein diacetate (CMFDA), 9′-(4-(and 5)-chloromethyl-2-carboxyphenyl)-7′-chloro-6′-oxo-1,2,2,4-tetramethyl-1,2-dihydropyrido[2′,3′-6]xanthene (CMRA), or 7-amino-4-chloromethylcoumarin (CMAC; 12.5μM; Invitrogen), following the manufacturer's protocol.

Platelet isolation and staining

Platelets were isolated from whole blood samples as described previously[25] and in supplemental Methods, and the purity of the sample confirmed with an ABX Pentra (Horiba). Platelets were counted in a Coulter counter (Beckman; 50-μm aperture tube, 3- to 30-fL particles), adjusted to 8×10^5 platelets/μL with washing buffer, and stained with PKH26 (Sigma-Aldrich) following the manufacturer's protocol. Platelets were centrifuged at 1250g at 22°C for 20 minutes and then adjusted to 9×10^6 (for in vivo experiments) or to 6×10^6 (for ex vivo experiments) platelets/μL in resuspension buffer.

Animals and drug treatments

All animal procedures were carried out in accordance with the United Kingdom Animals (Scientific Procedures) Act 1986 and following local ethic review.

SCID mice (CB17/ICR-*Prkdc^scid*/Crl) and C57BL/6J mice were purchased from Charles River Laboratories. *Cx₃cr1^gfp/+* and *Cx₃cr1^gfp/gfp* mice (B6.129P-*Cx3cr1^tm1Litt*/J) were obtained from The Jackson Laboratory.[30,31] C57Bl-6J/FVB/CD11b-diphtheria toxin receptor (DTR) and B6.Mac1-KO mice were gifts from Professor Martin Bennett, University of Cambridge, Cambridge, United Kingdom[32] and Professor Siamon Gordon, University of Oxford, Oxford, United Kingdom, respectively.[33]

Matrigel (growth factor reduced, BD Biosciences) was used for subcutaneous implantation of tumor cells in certain experiments.

Recombinant hirudin (Refludan; Pharmion) was administered intraperitoneally at 20 mg/kg,[22,23] 5 minutes before and 4 hours after the intravenous injection of tumor cells (and platelets) or on days 5 and 9 after the first signs of subcutaneous tumor growth.

Diphtheria toxin (DT; List Biological Laboratories) was administered intraperitoneally at 15 ng/g, on 2 consecutive days.

Anti–asialo-GM1 antibody (20 μL; Wako Chemicals GmbH) was administered intraperitoneally once a week for 3 weeks.[34]

For in vivo experiments, an intact lung imaging technique was performed, as described previously[25] and detailed in supplemental Meth-

ods. The isolated lung was inflated with 0.6 mL of air and remained inflated during the imaging.

Microscopy and image analysis

Images were acquired using an inverted epifluorescence microscope (DM IRB; Leica Microsystems) and a digital camera (Orca; Hamamatsu Photonics), and analyzed with Open Lab (Improvision; PerkinElmer Life and Analytical Sciences) and ImageJ Version 1.46 (http://rsb.info.nih.gov/ij) software.

Z-stack images were acquired with an inverted confocal microscope (LSM-710; Carl Zeiss Microimaging). The 32 PMT array of the confocal was used to record λ images, which were subsequently unmixed with Zen 2009 software using individually recorded spectra to remove inherent autofluorescence. Some images were acquired using an inverted confocal microscope (Radiance 2000-Nikon eclipse TE300; Bio-Rad and Nikon, respectively) and analyzed using LaserSharp 2000 (Bio-Rad) software. The objective lenses and the imaging setups for the different combinations of fluorophores are described in supplemental Methods. Image stacks of 30 to 50 slices with an interval of 1 to 1.5 μm of at least 10 random fields per lung were acquired. Maximum projections of the stacks are shown in the figures.

Volume of the clots associated with tumor cells were analyzed from z-series images. A slice containing the object of interest was selected and an appropriate threshold set to segment the object from the background. This threshold was then applied to the whole volume and the number of voxels in the object of interest calculated. Finally, voxels were converted into cubic micrometers according to the imaging setup.

Spatial heterogeneity of CX₃CR1-green fluorescent protein (GFP) cells was analyzed from maximum projection images obtained from z-series. The positions of local maxima above a threshold in the maximum projection image were used to represent the spatial distribution of the GFP cells. The degree to which the spatial distribution of these points deviated from a random Poisson distribution was quantified using Ripley K test.[35]

To score the number of cells in maximum projection images from z-series, the number of objects above a certain size limit and gray levels threshold was automatically counted.

Flow cytometry and immunohistochemistry

Single-cell suspensions from murine lung tissues were obtained as described in supplemental Methods. Surface levels of F4/80 (BM8; Invitrogen), CD11b (M1/70; eBioscience), Gr-1 (RB6-8C5; eBioscience), and NK-1.1 (PK136; eBioscience) on the lung cells were analyzed by flow cytometry performed on a FACSCalibur cytometer equipped with BD Cell Quest Version 6 software (BD Biosciences) and data analyzed with FlowJo Version 7.6.5 software.

Murine tissue sections were obtained as described in supplemental Methods, blocked and stained with the corresponding antibodies: rat anti-CD11b, rat anti-F4/80, rat anti-CD68, rat anti–Gr-1, and hamster anti-CD11c (all from Abcam), rat anti-CD45 and hamster anti-CD3ε (both from BD Biosciences Pharmingen), rat anti-integrin α_{IIb} (Santa Cruz Biotechnology), and goat anti-matrix metalloproteinase-9 (anti–MMP-9; R&D Systems). TSA biotin system amplification (PerkinElmer Life and Analytical Sciences) was performed using biotinylated secondary antibodies and streptavidin-conjugated fluorophores. Alkaline phosphatase-based amplification was performed using Polink-2 Plus AP Detection System (Golden Bridge International) and phosphatase substrate ELF97 (Invitrogen).

Statistical analysis

Statistical analysis was performed with GraphPad Prism Version 5.02, as described in supplemental Methods. The particular test performed in each experiment is indicated in the corresponding figure legend. Differences were considered significant with *P* less than .05. Data represent mean plus SD, unless specified otherwise.

Results

Clot formation by tumor cells in vivo leads to enhanced survival

TF triggers coagulation, but whether coagulation is critical for induction of metastasis by TF varies between different systems.[15,17,20] We first asked whether TF expression by tumor cells led to platelet clot formation. The A7 human melanoma cell line does not express TF. TF expression was induced by transfection of an expression vector to generate a stable population (A7/TF, Figure 1A).[8] A7 cells were associated with fewer and smaller platelet aggregates ex vivo than A7/TF cells (Figure 1B). In vivo, labeled platelets were used to visualize clots (previously shown to include both platelets and fibrin(ogen)[25]) surrounding A7 and A7/TF cells in the lung. Two hours after intravenous injection of the tumor cells, significantly more and larger clots were associated with A7/TF cells than with A7 cells (Figure 1C; supplemental Video 1).

Highly metastatic murine melanoma B16F10 cells express TF[11] (Figure 1A). Inhibition of TF in B16F10 cells with TFPI, an endogenous inhibitor of both the coagulative and the signaling activities of TF,[36] leads to metastatic failure.[11] Expression of TFPI in B16F10 cells (B16F10-TFPI) reduced clot formation on the tumor cells at 2 hours and 8 hours in vivo. By 24 hours, all of B16F10-wt cells, but none of the B16F10-TFPI, were surrounded by clots. Although TFPI expression reduced the percentage of cells with associated clots, it had little effect on the size of clots produced initially (2 hours; Figure 1D; and data not shown). We concluded that, in both these tumor cell lines, TF activity regulated platelet clot formation surrounding arrested tumor cells in the pulmonary circulation.

TF activity not only promotes clot formation but also tumor cell survival in the lungs. An equivalent number of either A7 (lacking TF) or A7/TF tumor cells were found in the lungs 2 hours after the injection (Figure 1E). However, by 24 hours, the survival of A7/TF cells was substantially greater than that of A7 cells, which were undetectable. Similarly, the survival of B16F10-wt cells was significantly higher than that of B16F10-TFPI. The decrease in cell number between 2 and 24 hours is an expected manifestation of metastatic inefficiency.

The effect of intracellular TF signaling on metastasis was tested by expressing TF lacking the cytoplasmic domain in A7 cells[8] (A7/TFΔCD; Figure 1A). The A7/TFΔCD cells were sorted to isolate populations with expression levels of the extracellular domain of TF similar to A7/TF cells (supplemental Figure 1A). An equivalent number of platelet aggregates formed ex vivo around A7/TFΔCD and A7/TF cells, although those surrounding A7/TFΔCD were slightly smaller in size (Figure 1B). Platelet clot formation in vivo and cell survival at 24 hours were not altered by the deletion of the cytoplasmic domain of TF (Figure 1C,E). We conclude that cellular signaling through TF does not contribute to early cancer cell survival in vivo.

Inhibition of clot formation with hirudin, a potent and selective inhibitor of thrombin, should not alter the initial interaction of TF with FVII and the intracellular signaling processes that depend only on TF. Treatment with hirudin resulted in not only a substantial decrease in clot formation but also reduced cell survival (8 hours) in the lung (Figure 1F; supplemental Figure 1B). We conclude that the coagulative activity of TF is crucial for early tumor cell survival in the lung.

Myeloid cells are recruited to tumor cells through clot formation

Clots are known to recruit macrophages in atherosclerotic plaques and after trauma.[37] Platelets mediate the recruitment of bone marrow-derived cells to hypoxic tissues to promote angiogenesis.[38] To ask whether tumor cell clot formation recruits macrophages, we visualized monocytes/macrophages using the CX$_3$CR1-GFP heterozygous mouse (*Cx$_3$cr1$^{gfp/+}$*, a GFP knock-in within the coding region of one allele of the fractalkine receptor, CX$_3$CR1, disrupting its expression). The predominant population of CX$_3$CR1-GFP$^+$ cells are myeloid derived.[30,31] From 30 minutes to 24 hours after B16F10 cell injection, lungs were isolated and imaged as intact organs. Initially after the injection, the distribution of the GFP$^+$ cells was homogeneous, but by 2 hours the GFP$^+$ cells started to group around the tumor cells and their clots. By 8 hours, clusters of myeloid cells were evident around the tumor cells. At 16 hours, the clusters started to dissolve; and by 24 hours, the overall distribution of the myeloid cells had returned to its original homogeneous pattern (Figure 2A). As these mice had been injected with labeled platelets to enable their detection, we verified that clusters of GFP$^+$ cells were also observed around the tumor cells in mice not injected with platelets (supplemental Figure 2A). We analyzed the distribution of GFP$^+$ cells with a Ripley test and confirmed the impression that clustering peaked at 8 hours and abated at 24 hours after the intravenous injection of the tumor cells (Figure 2A). At all time points, the GFP$^+$ cells were seen in continuity with the tumor cells via the clots, as if the clots were a bridge that brings together tumor cells and myeloid cells (Figure 2A; supplemental Videos 2-4). After the dispersal of the clusters, the tumor cells retained contact with a few GFP$^+$ cells (Figure 2A arrowheads). Thus, the initial cluster formation may serve to recruit cells of which a few then remain in contact with the tumor cell. Similar experiments in the CX$_3$CR1-GFP homozygous mouse (*Cx$_3$cr1$^{gfp/gfp}$*), which is completely deficient in CX$_3$CR1, showed that the fractalkine receptor was not essential for the formation of clots around the tumor cells, the recruitment of myeloid cells to the tumor cells, or tumor cell survival in the lung (Figure 2B).

To examine the relationship of clot formation to myeloid cell recruitment, we asked whether the prevention of clot formation led to alterations in myeloid recruitment. We inhibited TF by expression of TFPI, using B16F10-TFPI cells. We also inhibited the downstream key coagulant protein, thrombin, with hirudin. Both strategies resulted in a reduction in clustering of GFP$^+$ cells around tumor cells (Figure 2C; supplemental Figure 2B-C). Thus, platelet clot formation by arrested tumor cells was required for the subsequent myeloid cell recruitment.

Characterization of the recruited myeloid cells

The CX$_3$CR1-GFP$^+$ cells recruited to tumor cells could reflect a variety of myeloid cell types.[30,31] To determine the nature of these cells, we performed immunohistochemistry on sections of lungs that were harvested 8 hours after B16F10 injection, the time of maximal cluster formation by CX$_3$CR1-GFP cells. The majority of the recruited CX$_3$CR1-GFP cells stained for CD11b, but not for CD11c (Figure 3A). Overall, the majority of the GFP$^+$ cells in the clusters were CD11b, F4/80, and CD68 positive. They were rarely positive for Gr-1, a marker of granulocytes and myeloid derived suppressor cells; or CD3ε, a marker of lymphocytes. Staining for CD45 confirmed that the GFP$^+$ cells were immune cells (Figure 3B).
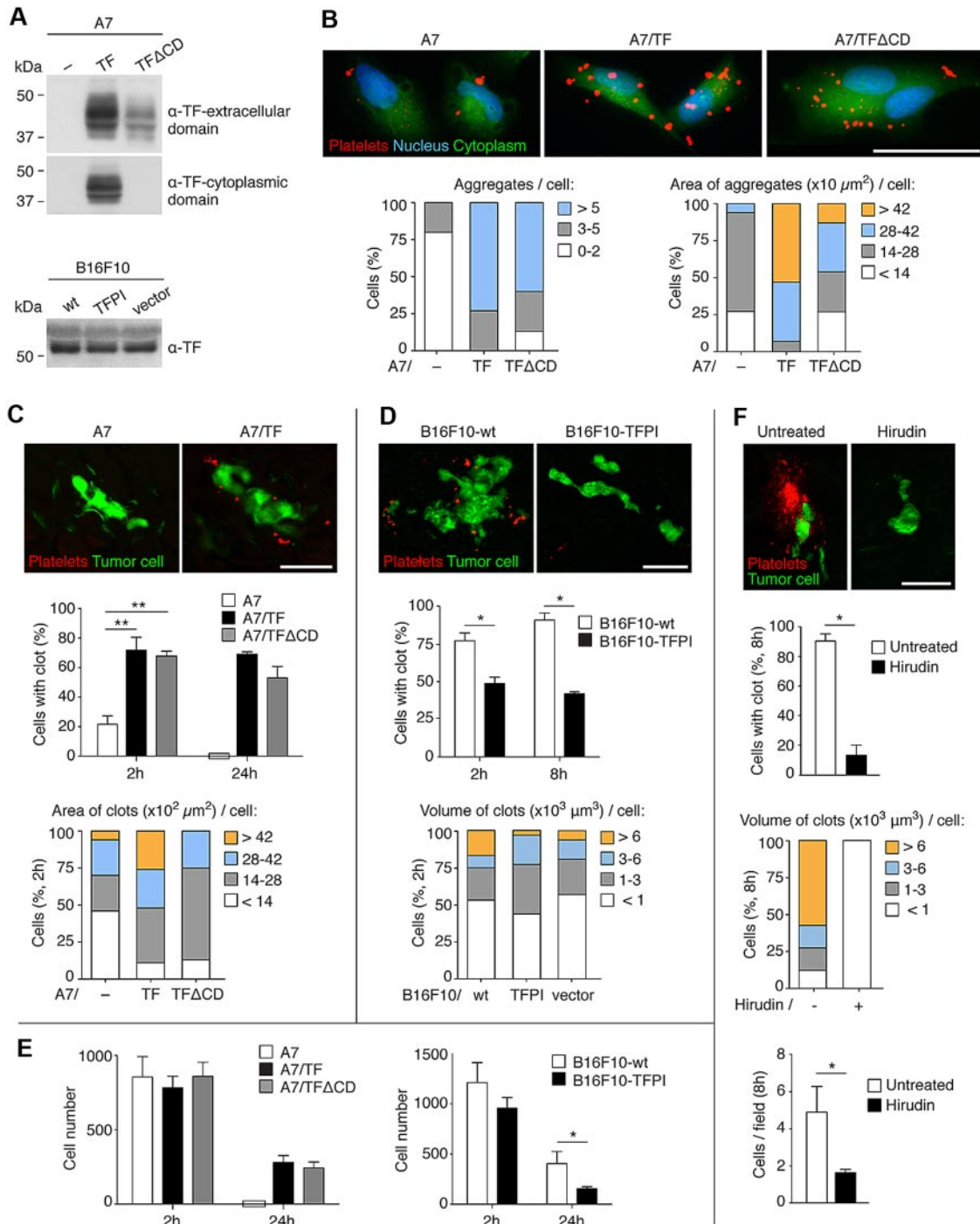
Figure 1. Clot formation induced by TF extracellular domain is essential for tumor cell survival. (A) Immunoblot detection of TF extracellular and cytoplasmic domains in extracts from human and murine melanoma cell lines. Representative Western blots from 3 independent experiments are shown. (B) Ex vivo assays of platelet aggregation. The 10^4 CMFDA-stained human melanoma cells (green) were seeded on collagen type I-biocoated multichamber slides. The 30×10^6 PKH26-stained platelets (red), isolated from SCID mice, were added and incubated for 2 hours. After fixation and 4,6-diamidino-2-phenylindole staining (blue), images were acquired with an epifluorescence microscope. Representative images of 1 of the 3 independent experiments performed are shown. Number and area of platelet aggregates associated with the cells were scored (15 cells per group were analyzed). (C-E) In vivo assays of clot formation (C-D) and cell survival assays (E). SCID (C and E left panels), $Cx_3cr1^{gfp/+}$ (D), or C57BL/6 (E right panel) mice were intravenously injected with 2.5×10^5 CMFDA-stained human melanoma cells (green, C and E left panels), or with 5×10^5 CMAC (green, D) or CMFDA (E right panel) stained murine melanoma cells and, on the opposite tail vein, with 9×10^9 PKH26-stained platelets (red), isolated from SCID (C) or C57BL/6 (D) mice. At the indicated times, lungs were isolated and imaged as intact organ with an epifluorescence (C,E) or a confocal (D) microscope. Representative images from the 2-hour time point, of 1 of the 3 independent experiments performed, are shown (C-D top panels). Tumor cell association with clots (C-D middle panels), the clot area or volume at the 2-hour time point (C-D bottom panels, ≥ 16 human and ≥ 30 murine cells with clot were analyzed), and the total number of tumor cells observed from images of consecutive fields of the entire left lobe of the lungs (E) were scored. n = 3 mice for panel C middle panel (1-way ANOVA and Tukey test for 2 hours, Mann-Whitney for 24 hours). n = 3 mice for panel D (middle panel; Mann-Whitney). n = 3 mice for panel E (1-way ANOVA, left panel 2 hours; Mann-Whitney, left panel 24 hours, and right panel). A χ^2 test showed a significant correlation ($P < 1.7 \times 10^{-16}$) between clot formation at 2 hours (C middle panel) and cell survival at 24 hours (E left panel). (F) $Cx_3cr1^{gfp/+}$ mice were treated with hirudin (20 mg/kg), given intraperitoneally 5 minutes before and 4 hours after the intravenous injection of 5×10^5 CMAC-stained B16F10-wt cells (green) and, on the opposite tail vein, 9×10^9 PKH26-stained platelets (red), isolated from C57BL/6 mice. Lungs were isolated after 8 hours and imaged as intact organ with a confocal microscope. Percentage of tumor cells with clot, volume of the clots (≥ 15 cells with clot were analyzed), and the total number of tumor cells per field were scored; n = 3 mice (Mann-Whitney). (C-F) Data are mean + SD. *$P < .05$. **$P < .01$. (B-D,F) Scale bars represent 50 μm.
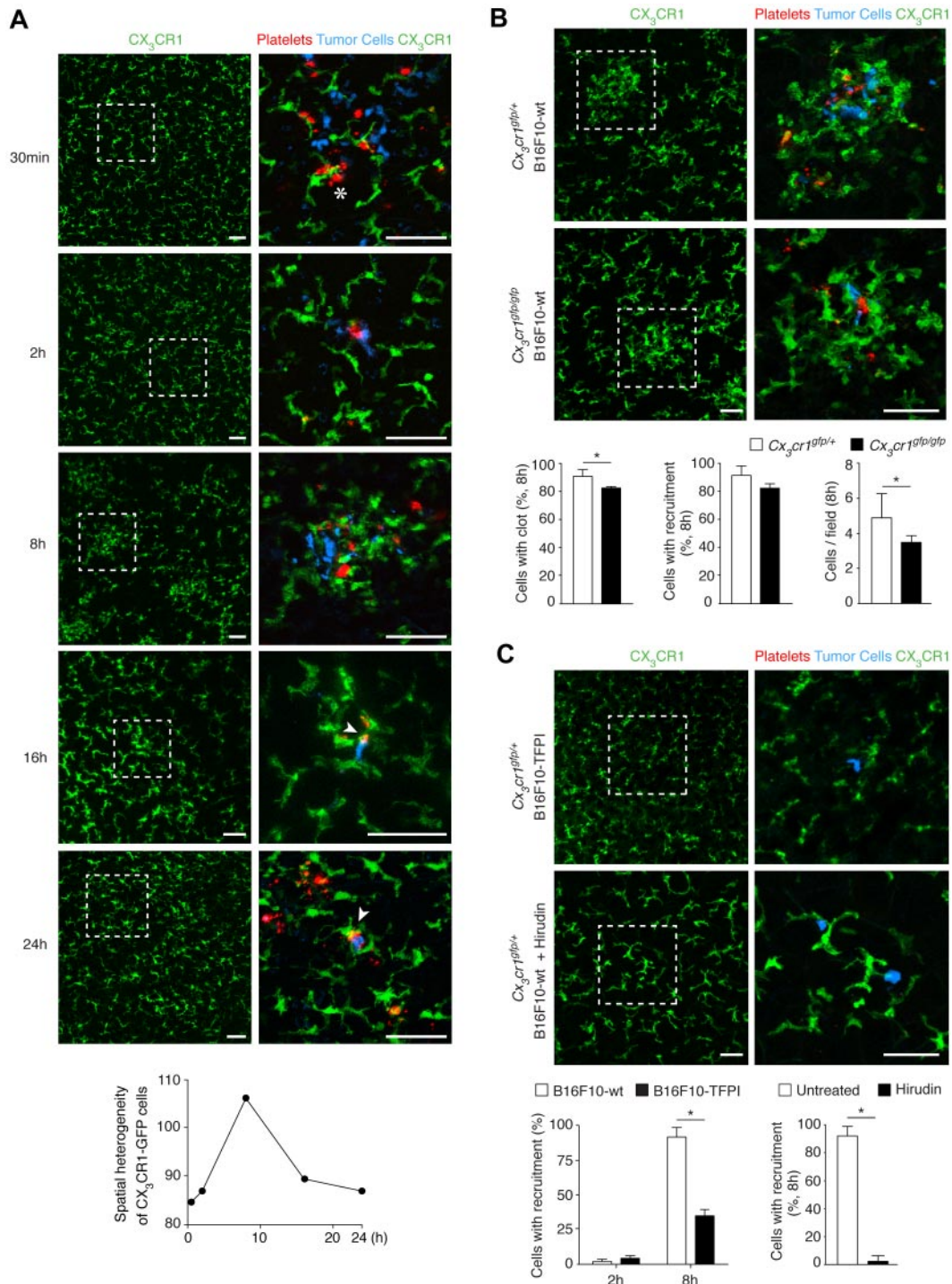
Figure 2. Recruitment of myeloid cells is mediated by tumor cell clot formation. (A) In vivo assays of myeloid cell (green) recruitment. $Cx_3cr1^{gfp/+}$ mice were intravenously injected with 5×10^5 CMAC-stained B16F10-wt cells (blue) and, on the opposite tail vein, with 9×10^9 PKH26-stained platelets (red), isolated from C57BL/6 mice. At the indicated times, lungs were isolated and imaged as intact organ with a confocal microscope. Arrowheads indicate direct contact between tumor cells and GFP+ cells. Occasionally, clots were also observed associated with myeloid cells (star). Representative images from 3 independent experiments performed per time point. Ripley test was performed to analyze clustering of CX_3CR1-GFP cells during the time course. y-axis represents the sum of K(r)/area (r) (K = Ripley K, r = distance range 5-100 pixels). Clustering of CX_3CR1-GFP cells around tumor cells, peaking at 8 hours, was observed in 2 other independent experiments. (B) The fractalkine receptor is not involved in recruitment to tumor cells. $Cx_3cr1^{gfp/+}$ (top panels) or $Cx_3cr1^{gfp/gfp}$ mice (middle panels) were intravenously injected with 5×10^5 CMAC-stained B16F10-wt cells (blue) and, on the opposite tail vein, with 9×10^9 PKH26-stained platelets (red), isolated from C57BL/6 mice. At 8 hours, lungs were isolated and imaged as intact organ with a confocal microscope. Representative images from 3 independent experiments performed are shown. Clot formation on tumor cells, recruitment of myeloid cells (green), and number of tumor cells observed per field were scored; n = 3 mice (Mann-Whitney). (C) Clot formation is required for subsequent myeloid cell recruitment. Myeloid cell (green) recruitment to tumor cells was assessed from images obtained from experiments described in Figure 1D and F. Representative images with B16F10-TFPI cells (blue; red, platelets; 8 hours after injection; top panels) and hirudin-treated mice (20 mg/kg; blue, tumor cell; red, platelets; middle panels) from 3 independent experiments are shown. Recruitment of myeloid cells to B16F10-wt and B16F10-TFPI tumor cells was scored at the indicated times (bottom left panel); n = 3 mice (Mann-Whitney). Recruitment of myeloid cells to tumor cells was scored in hirudin-treated mice (bottom right panel); n = 3 mice (Mann-Whitney). Scale bars represent 50 μm. White boxes define areas enlarged at right. (B-C) Data are mean + SD. *$P < .05$.

Figure 3. Characterization of the myeloid cells recruited to the tumor cells. (A) $Cx_3cr1^{gfp/+}$ mice were intravenously injected with 5×10^5 CMRA-stained B16F10-wt cells (blue). At 8 hours, lungs were isolated and analyzed by immunohistochemistry. Representative images, acquired with a confocal microscope, from a double staining for CD11b (red, ELF97) and CD11c (red, APC) are shown. The percentage of CX_3CR1-GFP cells within a cluster that coexpressed CD11b, CD11c, or both markers was analyzed; n = 3 mice; ≥ 10 clusters per mouse analyzed (1-way ANOVA and Tukey test). White boxes define areas enlarged in panels below. (B) Representative images, acquired with a confocal microscope, of sections from panel A stained for the presence of F4/80, CD68, Gr-1, CD3ε, and CD45 (all red, AlexaFluor-633) and the percentage of CX_3CR1-GFP cells within the clusters that coexpressed these markers; n = 3 mice; ≥ 10 clusters per mouse analyzed for each marker (1-way ANOVA and Tukey test). (A-B) Data are mean + SD. *$P < .05$. ***$P < .001$. Scale bars represent 50 μm.
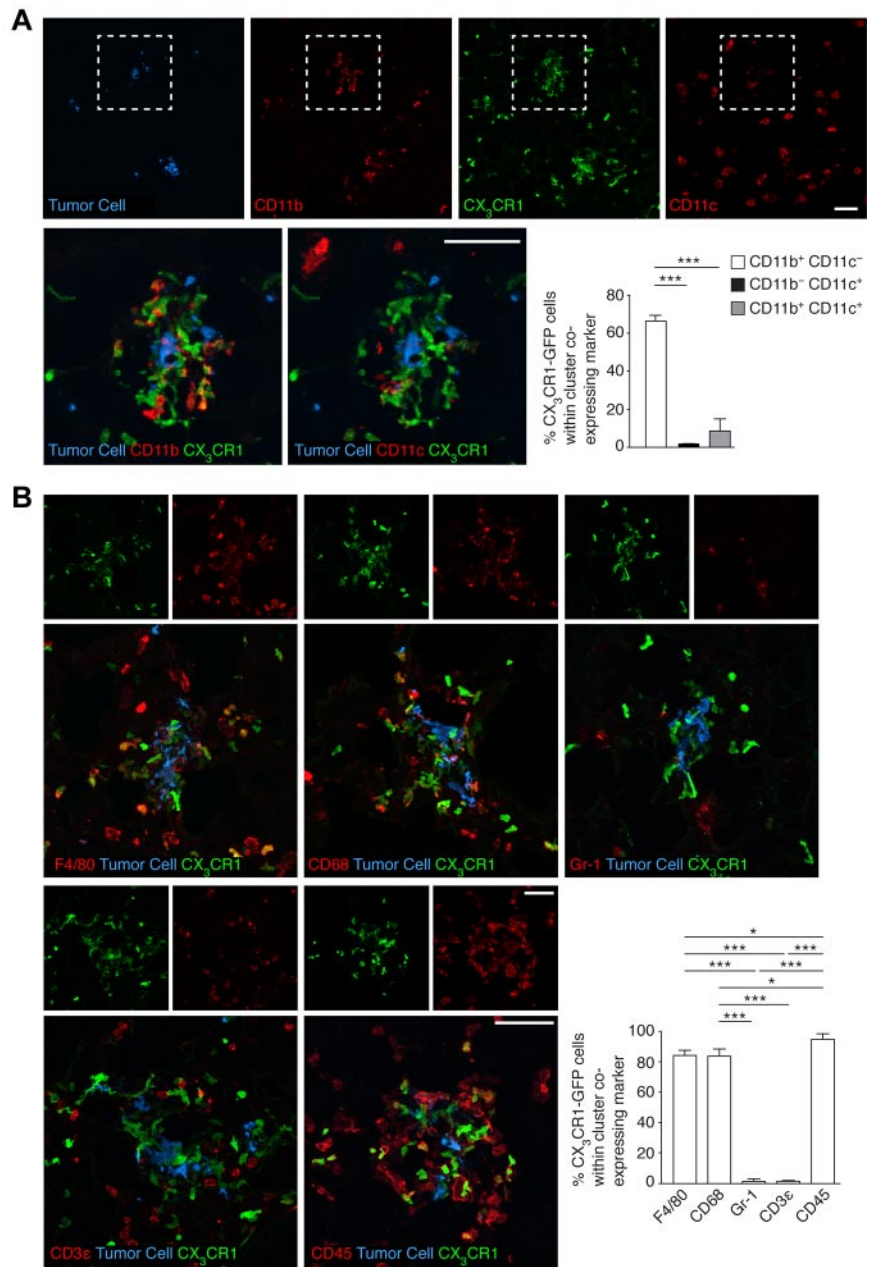
To extend these results, we tested cellular recruitment of CSF-1R-GFP^{+} myeloid cells in response to tumor cell arrest in mice.[39] After introduction of the syngeneic Met-1 cell line in *Csf1r-GFP* FVB mice, the majority of the clustered GFP^{+} cells were CD11b^{+}. Again, very few of the recruited cells had markers characteristic of dendritic, myeloid-derived suppressor, lymphoid cells, or neutrophils (supplemental Figure 3). Immunohistochemistry of lungs from C57BL/6 mice injected with B16F10 cells further confirmed that the clusters of cells surrounding the tumor cells were predominantly CD11b^{+} (Figure 4B). Clusters of CD11b^{+} cells also surrounded 4T1 murine breast and 1205Lu human melanoma cells in the pulmonary vasculature of BALB/c and SCID mice, respectively, 8 hours after intravenous injection (data not shown). Thus, the predominant recruited population is composed of CD11b^{+}, F4/80^{+}, CD68^{+}, CX_3CR1^+, CD11c^{−}, Gr-1^{−}, and CD3ε^{−} cells, consistent with a population of myeloid cells differentiated along the macrophage lineage.

Monocyte/macrophage recruitment is essential for tumor cell survival

To determine whether the platelet clots on the surface of the tumor cells per se or the subsequent recruitment of myeloid cells was responsible for the increase in tumor cell survival, we used 2 models in which the function of monocytes/macrophages was impaired. In the CD11b-DTR model, the CD11b promoter is linked to the human DTR,[32] conferring sensitivity to DT and permitting selective ablation of CD11b^{+} cells in vivo. Treatment with DT led to a substantial reduction in the population of CD11b^{+} cells within the myeloid gate. Depletion was evident in peripheral blood and in the lung, at the time of the injection of tumor cells and 8 hours later (Figure 4A). As previously reported, this treatment did not affect the neutrophil number, probably because of their relatively lower levels of CD11b expression.[32] Many fewer CD11b^{+} cells were present, but those remaining still formed smaller clusters around
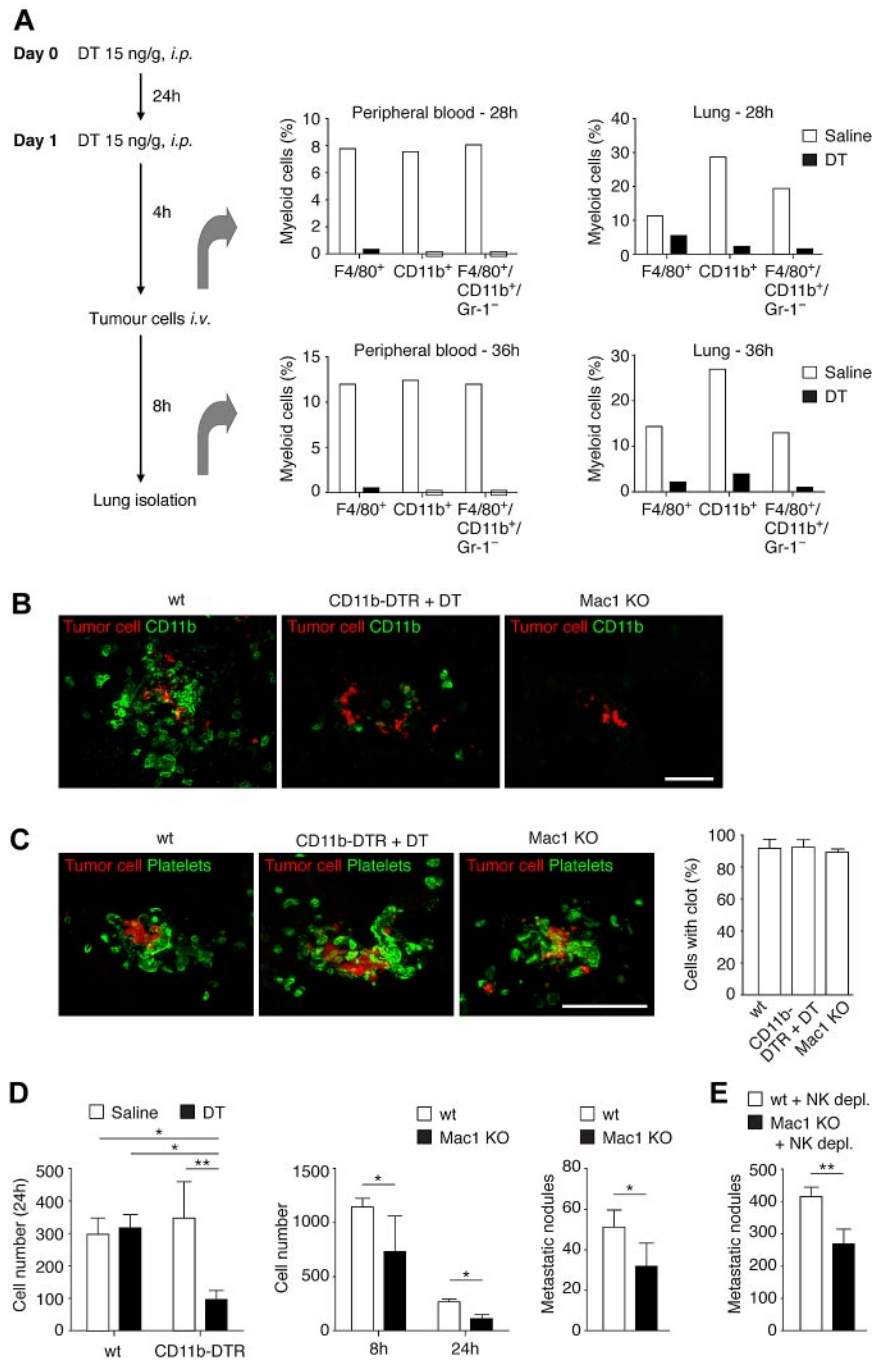
Figure 4. Impairment of macrophage function reduces tumor cell survival despite clot formation. (A) Experimental design for the ablation of macrophages in CD11b-DTR mice. DT was administered intraperitoneally (15 ng/g) on 2 consecutive days. Control mice were injected with saline at the same time points. Four hours after the second administration of DT or saline, 5×10^5 B16F10-wt cells were intravenously injected. The population of myeloid cells expressing F4/80, CD11b, and Gr-1 obtained at the time of the tumor cell injection or 8 hours after (as indicated), from either the peripheral blood or the lung, was analyzed by flow cytometry. (B-C) Immunohistochemistry against CD11b (B, AlexaFluor-488, green) and the platelet-specific integrin α_{IIb} (C, AlexaFluor-488, green) in lung sections from C57BL/6-wt or CD11b-DTR mice treated with DT as in panel A or Mac1 KO mice, 8 hours after intravenous injection of 5×10^5 CMRA-stained B16F10-wt cells (red, imaged with a confocal microscope). The percentage of tumor cells associated with platelets was scored; n = 3 mice, approximately 40 cells per mouse analyzed (1-way ANOVA). (D) Left panel: C57BL/6-wt or CD11b-DTR mice, treated as in panel A, were intravenously injected with 5×10^5 CMFDA-stained B16F10-wt cells. Lungs were isolated 24 hours after and imaged as intact organ with an epifluorescence microscope. The total number of tumor cells observed from images of consecutive fields of the entire left lobe of the lungs was scored; n = 3 mice (1-way ANOVA and Tukey test). Middle and right panels: C57BL/6-wt or Mac1 KO mice were intravenously injected with 5×10^5 CMFDA-stained (middle panel) or 2.5×10^5 unstained (right panel) B16F10-wt cells. Middle panel: Lungs were isolated 8 or 24 hours after tumor cell injection, imaged as intact organ with an epifluorescence microscope, and the number of tumor cells observed from images of consecutive fields of the entire left lobe of the lungs were scored; n ≥ 3 mice (Mann-Whitney). Right panel: Metastatic lung nodules were scored 3 weeks after intravenous injection of tumor cells; n ≥ 4 mice (Mann-Whitney). (E) NK-cell depletion assay. C57BL/6-wt or Mac1 KO mice were treated with anti–asialo-GM1 antibody (20 μL, intraperitoneally) on days 1, 8, and 15 and intravenously injected with 2.5×10^5 B16F10-wt cells on day 4. Lungs were isolated on day 25, and metastatic lung nodules were scored; n ≥ 4 mice (Mann-Whitney). (C-E) Data are mean + SD. *P < .05. **P < .01. (B-C) Scale bars represent 50 μm.

the tumor cells in the lung (Figure 4B). Platelet clots formed around the tumor cells in the DT-treated mice with a similar frequency to that in *wt* mice (Figure 4C). However, the tumor cell survival in the lung of the CD11b-DTR mice treated with DT was significantly decreased compared with CD11b-DTR mice treated with saline. DT treatment did not affect tumor cell survival in the lungs of *wt* mice (Figure 4D). Thus, platelet clot formation itself was not sufficient to confer survival on arrested tumor cells, but the ability of the clot to recruit CD11b+ cells was critical.

In the second model, we impaired monocyte/macrophage function using the Mac1 KO mouse, which lacks the α_M subunit (CD11b) of the Mac1 $\alpha_M\beta_2$ (CD11b/CD18) heterodimeric integrin[33] (Figure 4B). B16F10 cells formed platelet clots in the Mac1 KO mice to the same extent as in *wt* mice (Figure 4C). Fewer

CD45+ cells and virtually no F4/80+ cells were recruited to the tumor cells in Mac1 KO mice compared with *wt* (supplemental Figure 4A). Tumor cell survival in the lung was markedly reduced. Experimental metastasis assays confirmed a reduction in lung colonization by B16F10 cells in the Mac1 KO mouse (Figure 4D). Thus, tumor cell clot formation is not sufficient to provide tumor cell survival but requires the recruitment of functional CD11b+ cells.

Coagulation has been shown to protect tumor cells from NK activity.[20,27] To evaluate whether macrophages modulated NK-cell responses, we asked whether NK depletion was able to reverse the difference in metastasis between *wt* and Mac1-deficient mice. Treatment with anti–asialo-GM1 antibody reduced the number of NK cells in the lung by approximately 90% (supplemental Figure

Figure 5. Coagulation is required for the establishment of the premetastatic niche. (A) Experimental design to study the role of TF in the premetastatic niche. C57BL/6 mice were subcutaneously implanted with B16F10-wt cells and tumors allowed to grow for 21 days. Hirudin was administered intraperitoneally (20 mg/kg) 5 minutes before and 4 hours after intravenous injection of B16F10-wt cells. Lungs were isolated after either 24 hours or 14 days after intravenous injection to score for either cell survival or number of metastatic lung nodules, respectively. (B) Immunohistochemistry against CD11b (AlexaFluor-488, green) in lung sections 14 days after the subcutaneous implantation of 5×10^3 B16F10-wt tumor cells, before either intravenous injection or hirudin treatment. CD11b$^+$ cells per field were scored from tiled images, acquired with a confocal microscope, from naive and primary tumor-bearing mice; n = 3 mice, ≥ 15 single fields analyzed per mouse, extracted from ≥ 8 tiled images (Mann-Whitney). Scale bars represent 400 μm. (C) At 21 days after subcutaneous implantation of 5×10^3 B16F10-wt cells with Matrigel (growth factor-reduced), mice were treated with hirudin as described in panel A and intravenously injected with 2.5×10^5 CMFDA-stained B16F10-wt cells. Lungs isolated after 24 hours were sectioned, and the number of tumor cells per section was scored under an epifluorescence microscope; n = 3 mice, 9 nonconsecutive sections analyzed per mouse (Mann-Whitney). (D) At 21 days after subcutaneous implantation of 5×10^3 B16F10-wt cells, mice were treated with hirudin as described in panel A and intravenously injected with 2.5×10^5 unstained B16F10-wt cells. Lungs were isolated 14 days after and the number of metastatic lung nodules was scored; n = 3 mice (+s.c.; Mann-Whitney), n ≥ 9 mice (−s.c.; Mann-Whitney). (E-G) C57BL/6 mice were subcutaneously implanted with 5×10^3 B16F10-wt cells and pretreated with hirudin (20 mg/kg, intraperitoneally) on days 5 and 9 after palpable tumor growth (average of 12.6 days after implantation). On day 11, 2.5×10^5 B16F10-wt cells were intravenously injected, and lungs isolated 14 days later to score for metastatic lung nodules (F, n ≥ 5 mice, 1-way ANOVA and Tukey test). (G) The recruitment of CD11b cells to the premetastatic niche was analyzed by immunohistochemistry of lung sections from mice just before intravenous injection; n = 3 mice, ≥ 30 single fields analyzed per mouse (1-way ANOVA and Tukey test). (B-D,F-G) Data are mean + SD. *$P < .05$. **$P < .01$.
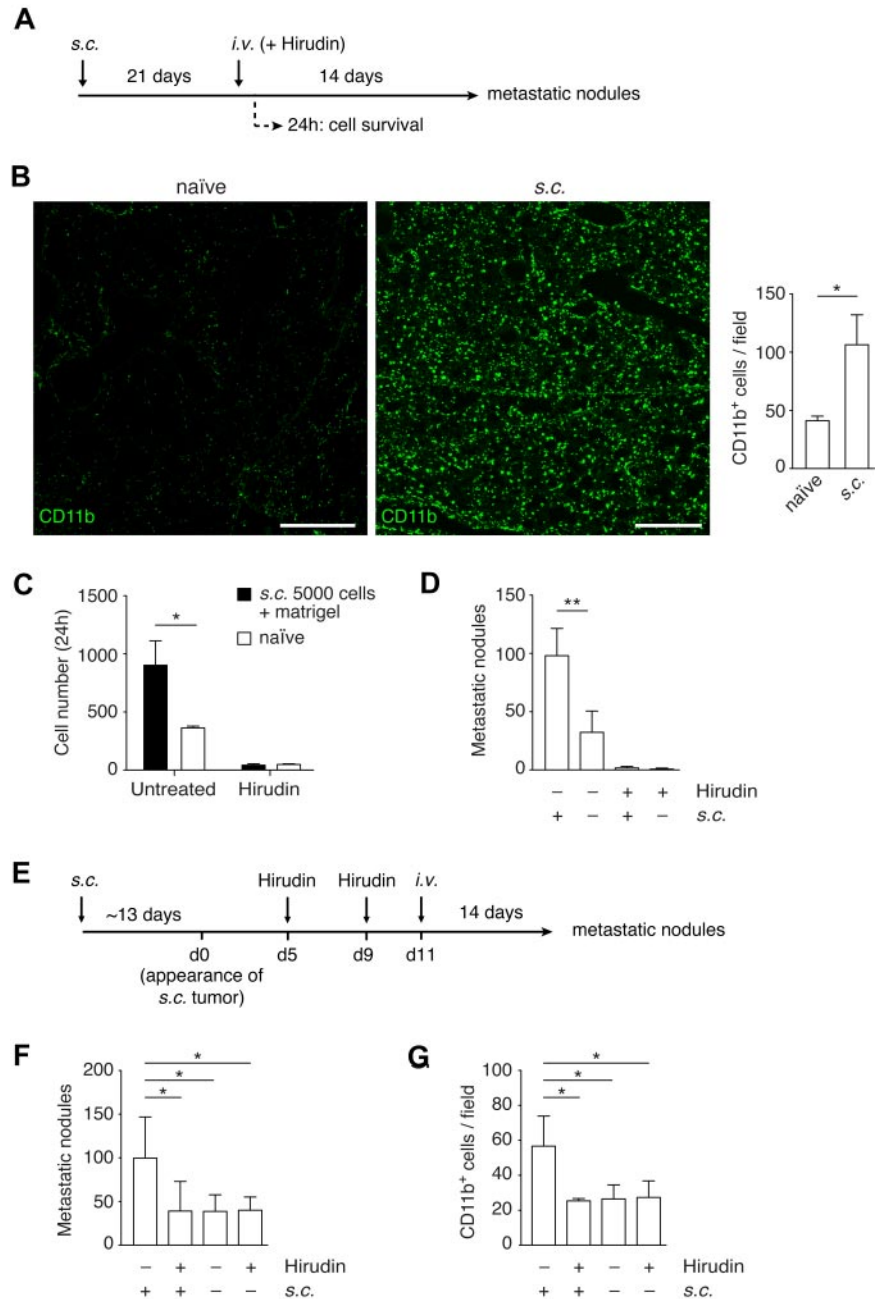
4B). NK depletion led to an increase in the number of metastatic lung nodules in both genotypes, but Mac1 KO mice remained with significantly and proportionally fewer metastatic lung nodules than *wt* mice. Moreover, the incidence of metastasis in nonpreferential organs, such as liver, ovary, kidney, and brain, was also less in Mac1 KO mice (supplemental Figure 4C). Thus, macrophage support of tumor cell survival in the lung appears to be independent of NK-cell activity (Figure 4E).

Coagulation is required for the establishment of the premetastatic niche

A primary tumor can generate a premetastatic niche, making distant sites more receptive to the development of metastasis. This phenomenon translates into an increase in the number of lung colonies, after intravenous introduction of tumor cells, in animals bearing a primary tumor compared with naive animals.[40-43]

Because this preconditioning results in increased numbers of CD11b$^+$ cells in the lungs,[40,41,43] we asked whether preconditioning can substitute for the functions provided by the coagulation-induced CD11b$^+$ cells clustered around tumor cells. The presence of a primary tumor resulted in an increase in the population of CD11b$^+$ cells and in MMP-9 (both cells and secreted protein) in the lung, as previously described[40,41] (Figure 5A-B; supplemental Figure 5A). This increase in CD11b cells was observed by 2 weeks after the tumor cell implantation, but not after 1 week (supplemental Figure 5B). We introduced B16F10 cells by intravenous injection into mice bearing B16F10 subcutaneous tumors (Figure 5A). Consistent with the formation of a premetastatic niche, the presence of a primary tumor led to an increase in B16F10 survival,

24 hours after intravenous injection (Figure 5C), and in the number of metastatic lung nodules (Figure 5D). We then asked whether preconditioning would reduce the inhibitory effect of anticoagulation on tumor cell survival. Treatment with hirudin at the time of intravenous injection of tumor cells reduced the number of surviving tumor cells and subsequent colony formation to the same level regardless of preconditioning (Figure 5C-D). Thus, formation of a premetastatic niche did not substitute for coagulation in the early events in lung colonization.

Finally, we investigated whether coagulation participates in the establishment of the premetastatic niche. Mice implanted with xenografts of B16F10-wt or B16F10-TFPI cells were treated with hirudin after palpable tumors were noted (Figure 5E). This design introduced hirudin after it would substantially alter tumor growth[23] (supplemental Figure 5C). Hirudin was withdrawn in time to restore coagulation before intravenous injection of the tumor cells. This protocol inhibited the establishment of a premetastatic niche, as defined by enhanced lung colonization. Pretreatment with hirudin in the absence of a premetastatic niche (naive mice) did not have any effect on the number of lung nodules (Figure 5F). The numbers of CD11b^{+} cells in the lungs were at control levels after pretreatment with hirudin (Figure 5G). Moreover, the involvement of coagulation in the establishment of the premetastatic niche was confirmed using the TF-deficient cell line, B16F10-TFPI. In this case, the presence of a primary tumor failed to enhance the numbers of lung colonies. Hirudin pretreatment of naive mice or of B16F10-TFPI tumor-bearing mice did not have a significant effect on the number of metastatic lung nodules or on the level of CD11b^{+} cells in the lung (supplemental Figure 5D-E).

To further characterize the cells recruited to the premetastatic niche, we implanted xenografts of B16F10 cells in CX$_3$CR1-GFP heterozygous mice. We found an increase in the population of GFP cells in mice with a primary tumor and that these GFP cells tended to be found in clusters (Figure 6A). Eight hours after intravenous injection of tumor cells in preconditioned mice, 87% of the tumor cells were surrounded by platelet clots and 84% by clusters of GFP cells. However, 24 hours later, as had been observed in naive mice, those clusters had abated (Figure 6B). We characterized the GFP^{+} cells in the clusters and observed that they were mainly CD11b^{+}, CD11c^{−}, CD68^{+}, Gr-1^{−}, and CD3ε^{−}, similar to those identified surrounding tumor cells previously in naive mice (Figure 6C).

Discussion

A body of evidence shows that the expression of TF by cancer cells, as well as other procoagulant factors, enhances their metastatic capacity.[3] An independent body of evidence shows that monocytes/macrophages are essential for effective metastasis.[44] Our work, for the first time, links TF-induced coagulation to macrophage recruitment in the metastatic process. Failure to form platelet clots around tumor cells led to decreased macrophage recruitment and impaired tumor cell survival. Clot formation without recruitment of functional macrophages was not sufficient to support tumor cell survival. Finally, inhibition of clot formation also prevented the formation of a premetastatic niche and its associated recruitment of monocytes/macrophages to the lungs (Figure 7).

We have altered tumor cell-induced clot formation with 3 different approaches: expression of TF in TF-deficient cells (A7), expression of the primary regulator of TF, TFPI, in cells proficient for TF (B16F10), and inhibition of the downstream key procoagulant enzyme, thrombin, with hirudin. All 3 strategies,

genetic and pharmacologic, have led to the same conclusion: clot formation by the tumor cells is essential for their survival in the lung in the early stages of metastasis. Consistent with these results, deletion of the cytoplasmic domain of TF in A7/TFΔCD cells, which did not affect the procoagulant activity of TF, did not reduce tumor cell survival in the lung. Our data are in agreement with previous observations, in which an absence of the cytoplasmic domain did not alter the metastatic potential to the lung, but the entire lack of TF led to metastatic failure.[20] During tumor growth, however, signaling through the cytoplasmic domain, leading to PAR2 activation through TF-VIIa–mediated cleavage, can play a crucial role.[9,15,17,19] Thus, the effect of TF in promoting metastatic tumor cell survival is linked to its capacity to induce clot formation on the tumor cell and not to intracellular events that depend on the cytoplasmic domain. To investigate how these clots promote tumor cell survival, we studied their possible interaction with myeloid cells because clots are well known to be able to recruit monocytes/macrophages.[37,38]

To show that platelet clot formation led to myeloid cell recruitment, we used 2 approaches: inhibition of tumor cell TF with TFPI and inhibition of thrombin with hirudin. Both strategies led to reduced clustering of macrophages. Intracellular signaling dependent on TF should continue, even in the presence of hirudin, indicating that this signaling is not sufficient to trigger the recruitment. To determine whether monocyte/macrophage recruitment contributed to metastasis, we examined 2 models with impaired function of monocytes/macrophages. Tumor cells still induced platelet clot formation in both these models, but tumor cell survival was diminished. These experiments showed that clot formation per se was not sufficient to provide tumor cell survival but required the subsequent recruitment of functional monocytes/macrophages. Thus, the recruitment of macrophages directed by coagulation induced by tumor cell TF is an integral part of metastasis initiation. It has been shown recently that TF expression by host stromal cells, including myeloid and endothelial cells, does not play a critical role in tumor growth.[45] Whether TF expression in the host is relevant for the metastatic process needs further investigation. However, these experiments provide some clues as to the mechanism by which platelet clots recruit and retain macrophages. Macrophage recruitment to tumor cells was decreased in Mac1-deficient mice, suggesting that macrophage CD11b plays a role. Mac1 is critical for myelomonocytic cell recruitment to sites of inflammation. The integrin CD11b can bind to clot components, such as platelet glycoprotein Ibα and fibrin,[46] as well as activated endothelium. Selectins have been shown to participate in the interactions between cancer cells, platelets, and leukocytes. Laubli et al showed that a coculture of tumor cells expressing P-selectin ligand, leukocytes, and platelets led to endothelial cell activation and induction of CCL5, whose inhibition in vivo was able to attenuate metastasis.[28] Thus, tumor cells are able to trigger coagulation by different means with overlapping, but not identical, consequences.

Coagulation has been implicated in metastasis through protection of tumor cells from NK cells. Palumbo et al[20,27] showed that TF confers metastatic potential, even in the absence of NK cells. They postulated the existence of at least 1 additional mechanism, prothrombin-dependent and NK-independent, by which tumor cell-associated TF supported the stable adhesion/survival of tumor cells in the lungs.[20,27] Our experiments implicate monocytes/macrophages recruited by clots as one potential NK-independent mechanism.
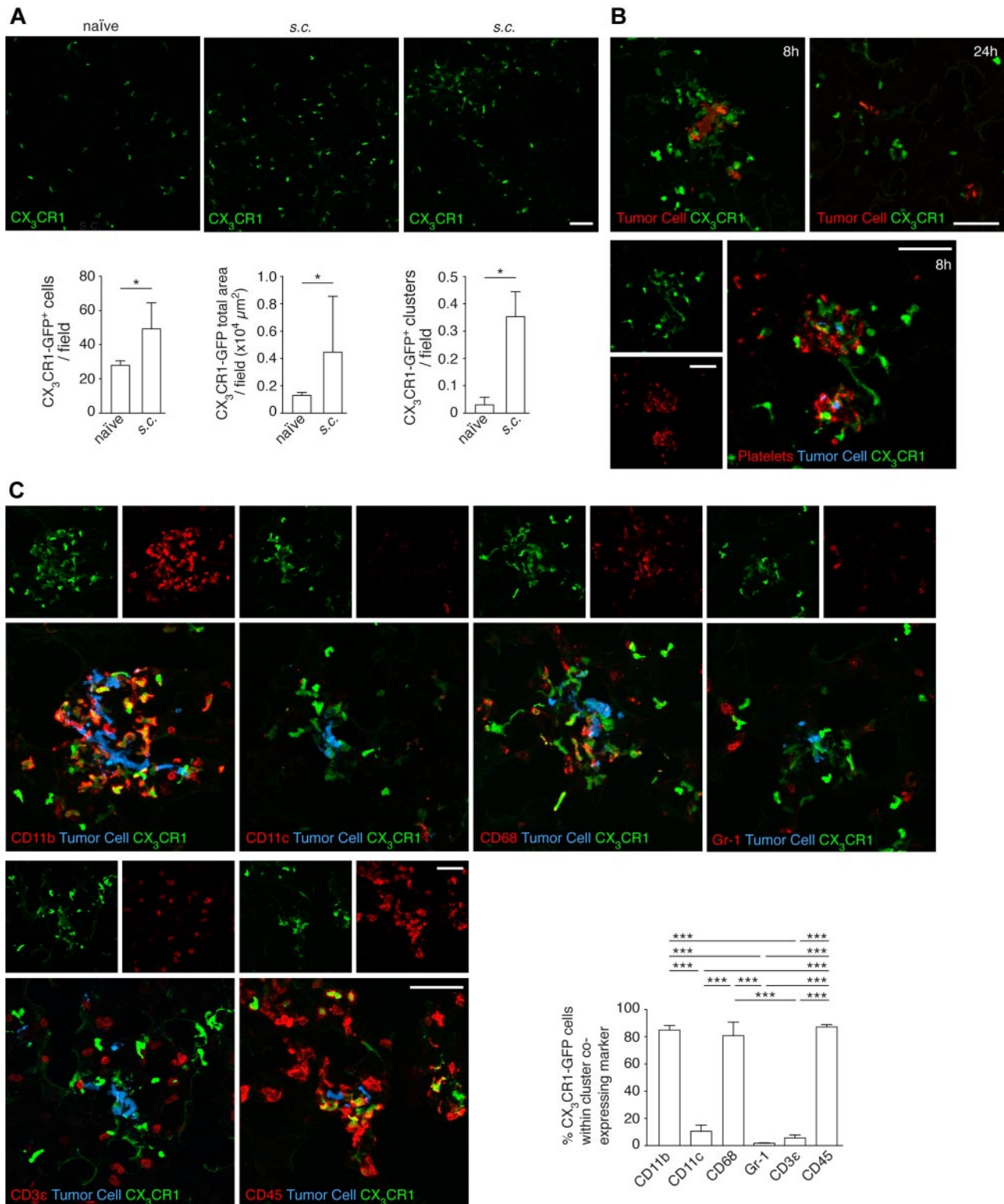
Figure 6. Characterization of the myeloid cells recruited to the premetastatic niche. (A) $Cx_3cr1^{gfp/+}$ mice were subcutaneously injected with 5×10^3 B16F10 cells. After 21 days, lungs were isolated and sections imaged with a confocal microscope (top panels) and scored by software for the number (bottom left) and area (bottom middle) of CX_3CR1-GFP cells per field; n = 3 mice, ≥ 35 single fields analyzed per mouse (Mann-Whitney). The number of CX_3CR1-GFP cell clusters (as seen in top right panel) per field was manually scored (bottom right); n = 3 mice, ≥ 35 single fields analyzed per mouse (Mann-Whitney). (B) $Cx_3cr1^{gfp/+}$ mice were intravenously injected with 5×10^5 CMRA-stained B16F10-wt cells after the establishment of the premetastatic niche, as described in panel A. Lungs, isolated either 8 or 24 hours after intravenous injection of tumor cells, were sectioned and directly imaged with a confocal microscope (top panels, tumor cell in red) or after immunohistochemistry (bottom panels) against the platelet-specific integrin α_{IIb} (AlexaFluor-633, red; and tumor cells, blue; 8 hours only). Representative images from 3 independent experiments performed per time point are shown. (C) Immunohistochemistry of sections from panel B, imaged with a confocal microscope (8 hours after the intravenous injection of tumor cells) against CD11b, CD11c, CD68, Gr-1, CD3ε, and CD45 (AlexaFluor-633, red; and tumor cells, blue). The percentage of CX_3CR1-GFP cells within the clusters that coexpressed the indicated markers was scored; n = 3 mice, ≥ 10 clusters analyzed per mouse (1-way ANOVA and Tukey test). Scale bars represent 50 μm. (A,C) Data are mean + SD. *$P < .05$. ***$P < .001$.
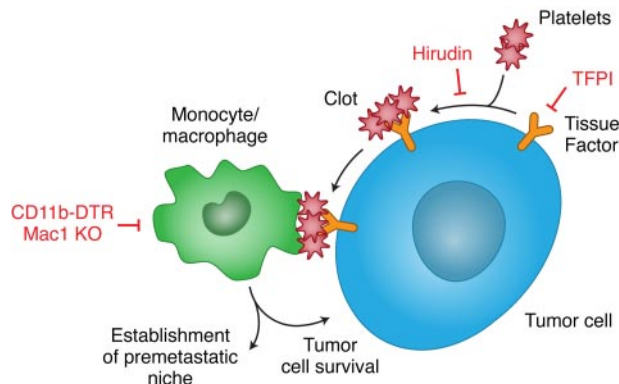
Figure 7. Recruitment of myeloid cells by TF-induced coagulation promotes metastasis. TF expressed in cancer cells triggers the coagulation cascade that results in thrombin formation, platelet activation, and fibrin deposition. The clots formed on the tumor cells serve to recruit a subset of monocytes/macrophages that are essential for in vivo tumor cell survival and for the establishment of a premetastatic niche. Prevention of clot formation, by inhibition of either TF (with TFPI) or thrombin (with hirudin), results in a decreased recruitment of monocytes/macrophages that perturbs tumor cell survival and the establishment of a premetastatic niche. Impairment of monocyte/macrophage function, in mice depleted of CD11b cells or in Mac1 KO mice, leads to the same consequences, despite the formation of clots on the tumor cells. Thus, TF and the monocyes/macrophages it recruits are potentially interesting targets in the treatment and prophylaxis of metastases.

Historically, macrophages were considered to exclusively exert an antitumoral activity. It is now recognized that macrophages also enhance tumorigenesis and progression.[44,47] Qian et al have shown that ablation of macrophages at the time of intravenous injection of tumor cells leads to depressed numbers of lung colonies.[39] They also observed that recruitment to the lung of a population of macrophages,[39] similar to the one we have found, by tumor cells, was dependent on CCL2.[48] The possibly differing roles of the initial cluster or the subsequent direct contact with the tumor cells remain to be elucidated. It is plausible that several waves of recruitment of monocytes/macrophages occur, being the first wave coagulation-dependent and responsible for the initial survival of tumor cells in the pulmonary capillaries. A recent report from Chen et al[49] shows that aberrant expression of VCAM-1 in breast cancer cells serves to interact directly with macrophages via α4 integrins and triggers a signaling pathway that results in tumor cell survival, by counteracting proapoptotic signals dependent on TRAIL. Another possibility is that tumor cell survival depends on chemokines or cytokines secreted by the recruited macrophages. The second wave, on the other hand, is unlikely to be coagulation-dependent because later administration of anticoagulants does not have an effect on metastasis and could be, instead, responsible for extravasation, as reported by Qian et al.[39]

Systemic changes arise in response to primary tumor growth and prime distant tissues for tumor cell implantation and proliferation.[40,43] These are characterized by recruitment of bone marrow-derived progenitor cells that express, among other markers, CD11b.[40,41,43] Deposition of fibronectin,[43] expression of MMP-9,[40,43] and lysil-oxidase activity[50] in premetastatic niches have also been observed. We explored the role of coagulation in this process, using the aforementioned approaches: inhibition of TF with TFPI and inhibition of thrombin with hirudin. First, we show that the increase in CD11b+ cells in the lung associated with the premetastatic niche is not sufficient in itself to promote tumor cell survival. Coagulation and CD11b+ clustering were still required. Second, we asked

whether the recruitment of CD11b+ cells in the premetastatic niche was coagulation dependent. We found that that was the case. Interestingly, macrophages recruited to the lung during the formation of a premetastatic niche had the same markers as those attracted to the tumor cells via clot formation soon after arrest in the lung. Thus, there are several means through which anticoagulation might inhibit metastasis, both through decreased survival at the targeted site and failure to form a premetastatic niche.

We propose that, in TF-expressing tumor cells, TF triggers the formation of a platelet clot around the tumor cells soon after arrest at a distant site. The clot then triggers the localization of monocytes/macrophages to the tumor cells. These macrophages are required for survival of the tumor cell. Therefore, tumor cell TF can contribute to the metastatic process by initiation of a cellular process that results in the recruitment of macrophages to the tumor cell. Likewise, coagulation is required for the recruitment of a similar subset of monocytes/macrophages to distant sites in which circulating tumor cells settle and prosper. The dramatic reduction in lung metastasis provided by interruption of this succession of events opens an interesting therapeutic (and even prophylactic) opportunity in the treatment of metastasis.

Authorship

Contribution: A.M.G.-B. designed and performed research, analyzed and interpreted data, performed statistical analysis, and wrote the manuscript; S.F. and L.Z. performed research; M.T., J.H.I., K.W., and S.A.H. provided expert assistance; P.D.A. analyzed data; A.A., J.L.F., J.W.P., and W.R. provided relevant material; W.R. edited the manuscript and provided expert advice; and R.J.M. designed research, analyzed and interpreted data, and wrote the manuscript.

Conflict-of-interest disclosure: The authors declare no competing financial interests.

Correspondence: Ruth J. Muschel, Gray Institute for Radiation Oncology and Biology, ORCRB, Roosevelt Drive, Oxford, OX3 7DQ, United Kingdom; e-mail: ruth.muschel@gmail.com.

References

1. Falanga A, Panova-Noeva M, Russo L. Proco-agulant mechanisms in tumour cells. *Best Pract Res Clin Haematol.* 2009;22(1):49-60.

2. Laubli H, Borsig L. Selectins promote tumor metastasis. *Semin Cancer Biol.* 2010;20(3):169-177.

3. Palumbo JS, Degen JL. Mechanisms linking tumor cell-associated procoagulant function to tumor metastasis. *Thromb Res.* 2007;120(suppl 2):S22-S28.

4. Versteeg HH, Ruf W. Emerging insights in tissue factor-dependent signaling events. *Semin Thromb Hemost.* 2006;32(1):24-32.

5. Abe K, Shoji M, Chen J, et al. Regulation of vascular endothelial growth factor production and angiogenesis by the cytoplasmic tail of tissue factor. *Proc Natl Acad Sci U S A.* 1999;96(15):8663-8668.

6. Belting M, Dorrell MI, Sandgren S, et al. Regulation of angiogenesis by tissue factor cytoplasmic domain signaling. *Nat Med.* 2004;10(5):502-509.

7. Versteeg HH, Schaffner F, Kerver M, et al. Inhibition of tissue factor signaling suppresses tumor growth. *Blood.* 2008;111(1):190-199.

8. Dorfleutner A, Hintermann E, Tarui T, Takada Y, Ruf W. Cross-talk of integrin alpha3beta1 and tissue factor in cell migration. *Mol Biol Cell.* 2004;15(10):4416-4425.

9. Schaffner F, Versteeg HH, Schillert A, et al. Cooperation of tissue factor cytoplasmic domain and PAR2 signaling in breast cancer development. *Blood.* 2010;116(26):6106-6113.

10. Milsom C, Rak J. Tissue factor and cancer. *Pathophysiol Haemost Thromb.* 2008;36(3):160-176.

11. Amirkhosravi A, Meyer T, Chang JY, et al. Tissue factor pathway inhibitor reduces experimental lung metastasis of B16 melanoma. *Thromb Haemost.* 2002;87(6):930-936.

12. Hembrough TA, Swartz GM, Papathanassiu A, et al. Tissue factor/factor VIIa inhibitors block angiogenesis and tumor growth through a nonhemostatic mechanism. *Cancer Res.* 2003;63(11):2997-3000.

13. Milsom CC, Yu JL, Mackman N, et al. Tissue factor regulation by epidermal growth factor receptor and epithelial-to-mesenchymal transitions: effect on tumor initiation and angiogenesis. *Cancer Res.* 2008;68(24):10068-10076.

14. Mueller BM, Reisfeld RA, Edgington TS, Ruf W. Expression of tissue factor by melanoma cells promotes efficient hematogenous metastasis. *Proc Natl Acad Sci U S A.* 1992;89(24):11832-11836.

15. Mueller BM, Ruf W. Requirement for binding of catalytically active factor VIIa in tissue factor-dependent experimental metastasis. *J Clin Invest.* 1998;101(7):1372-1378.

16. Ngo CV, Picha K, McCabe F, et al. CNTO 859, a humanized anti-tissue factor monoclonal antibody, is a potent inhibitor of breast cancer metastasis and tumor growth in xenograft models. *Int J Cancer.* 2007;120(6):1261-1267.

17. Bromberg ME, Konigsberg WH, Madison JF, Pawashe A, Garen A. Tissue factor promotes melanoma metastasis by a pathway independent of blood coagulation. *Proc Natl Acad Sci U S A.* 1995;92(18):8205-8209.

18. Milsom C, Anderson GM, Weitz JI, Rak J. Elevated tissue factor procoagulant activity in CD133-positive cancer cells. *J Thromb Haemost.* 2007;5(12):2550-2552.

19. Bromberg ME, Sundaram R, Homer RJ, Garen A, Konigsberg WH. Role of tissue factor in metastasis: functions of the cytoplasmic and extracellular domains of the molecule. *Thromb Haemost.* 1999;82(1):88-92.

20. Palumbo JS, Talmage KE, Massari JV, et al. Tumor cell-associated tissue factor and circulating hemostatic factors cooperate to increase metastatic potential through natural killer cell-dependent and-independent mechanisms. *Blood.* 2007;110(1):133-141.

21. Nierodzik ML, Karpatkin S. Thrombin induces tumor growth, metastasis, and angiogenesis: evidence for a thrombin-regulated dormant tumor phenotype. *Cancer Cell.* 2006;10(5):355-362.

22. Esumi N, Fan D, Fidler IJ. Inhibition of murine melanoma experimental metastasis by recombinant desulfatohirudin, a highly specific thrombin inhibitor. *Cancer Res.* 1991;51(17):4549-4556.

23. Hu L, Lee M, Campbell W, Perez-Soler R, Karpatkin S. Role of endogenous thrombin in tumor implantation, seeding, and spontaneous metastasis. *Blood.* 2004;104(9):2746-2751.

24. Horowitz NA, Blevins EA, Miller WM, et al. Thrombomodulin is a determinant of metastasis through a mechanism linked to the thrombin binding domain but not the lectin-like domain. *Blood.* 2011;118(10):2889-2895.

25. Im JH, Fu W, Wang H, et al. Coagulation facilitates tumor cell spreading in the pulmonary vasculature during early metastatic colony formation. *Cancer Res.* 2004;64(23):8613-8619.

26. Nieswandt B, Hafner M, Echtenacher B, Mannel DN. Lysis of tumor cells by natural killer cells in mice is impeded by platelets. *Cancer Res.* 1999;59(6):1295-1300.

27. Palumbo JS, Talmage KE, Massari JV, et al. Platelets and fibrin(ogen) increase metastatic potential by impeding natural killer cell-mediated elimination of tumor cells. *Blood.* 2005;105(1):178-185.

28. Laubli H, Spanaus KS, Borsig L. Selectin-mediated activation of endothelial cells induces expression of CCL5 and promotes metastasis through recruitment of monocytes. *Blood.* 2009;114(20):4583-4591.

29. Labelle M, Begum S, Hynes RO. Direct signaling between platelets and cancer cells induces an epithelial-mesenchymal-like transition and promotes metastasis. *Cancer Cell.* 2011;20(5):576-590.

30. Auffray C, Fogg D, Garfa M, et al. Monitoring of blood vessels and tissues by a population of monocytes with patrolling behavior. *Science.* 2007;317(5838):666-670.

31. Jung S, Aliberti J, Graemmel P, et al. Analysis of fractalkine receptor CX(3)CR1 function by targeted deletion and green fluorescent protein reporter gene insertion. *Mol Cell Biol.* 2000;20(11):4106-4114.

32. Stoneman V, Braganza D, Figg N, et al. Monocyte/macrophage suppression in CD11b diphtheria toxin receptor transgenic mice differentially affects atherogenesis and established plaques. *Circ Res.* 2007;100(6):884-893.

33. Coxon A, Rieu P, Barkalow FJ, et al. A novel role for the beta 2 integrin CD11b/CD18 in neutrophil apoptosis: a homeostatic mechanism in inflammation. *Immunity.* 1996;5(6):653-666.

34. Winkler-Pickett R, Young HA, Cherry JM, et al. In vivo regulation of experimental autoimmune encephalomyelitis by NK cells: alteration of primary adaptive responses. *J Immunol.* 2008;180(7):4495-4506.

35. Dixon PM. Ripley's K function. In: El-Shaarawi AH, Piegorsch WW, eds. *Encyclopedia of Environmetrics.* Vol. 3. Chichester, United Kingdom: John Wiley & Sons; 2002:1796-1803.

36. Ahamed J, Belting M, Ruf W. Regulation of tissue factor-induced signaling by endogenous and recombinant tissue factor pathway inhibitor 1. *Blood.* 2005;105(6):2384-2391.

37. Gautier EL, Jakubzick C, Randolph GJ. Regulation of the migration and survival of monocyte subsets by chemokine receptors and its relevance to atherosclerosis. *Arterioscler Thromb Vasc Biol.* 2009;29(10):1412-1418.

38. Feng W, Madajka M, Kerr BA, Mahabeleshwar GH, Whiteheart SW, Byzova TV. A novel role for platelet secretion in angiogenesis: mediating bone marrow-derived cell mobilization and homing. *Blood.* 2011;117(14):3893-3902.

39. Qian B, Deng Y, Im JH, et al. A distinct macrophage population mediates metastatic breast cancer cell extravasation, establishment and growth. *PLoS One.* 2009;4(8):e6562.

40. Hiratsuka S, Nakamura K, Iwai S, et al. MMP9 induction by vascular endothelial growth factor receptor-1 is involved in lung-specific metastasis. *Cancer Cell.* 2002;2(4):289-300.

41. Hiratsuka S, Watanabe A, Aburatani H, Maru Y. Tumour-mediated upregulation of chemoattractants and recruitment of myeloid cells predetermines lung metastasis. *Nat Cell Biol.* 2006;8(12):1369-1375.

42. Hiratsuka S, Watanabe A, Sakurai Y, et al. The S100A8-serum amyloid A3-TLR4 paracrine cascade establishes a pre-metastatic phase. *Nat Cell Biol.* 2008;10(11):1349-1355.

43. Kaplan RN, Riba RD, Zacharoulis S, et al. VEGFR1-positive haematopoietic bone marrow progenitors initiate the pre-metastatic niche. *Nature.* 2005;438(7069):820-827.

44. Condeelis J, Pollard JW. Macrophages: obligate partners for tumor cell migration, invasion, and metastasis. *Cell.* 2006;124(2):263-266.

45. Liu Y, Jiang P, Capkova K, et al. Tissue factor-activated coagulation cascade in the tumor microenvironment is critical for tumor progression and an effective target for therapy. *Cancer Res.* 2011;71(20):6492-6502.

46. Simon DI, Chen Z, Xu H, et al. Platelet glycoprotein ibalpha is a counterreceptor for the leukocyte integrin Mac-1 (CD11b/CD18). *J Exp Med.* 2000;192(2):193-204.

47. Hanahan D, Weinberg RA. Hallmarks of cancer: the next generation. *Cell.* 2011;144(5):646-674.

48. Qian BZ, Li J, Zhang H, et al. CCL2 recruits inflammatory monocytes to facilitate breast-tumour metastasis. *Nature.* 2011;475(7355):222-225.

49. Chen Q, Zhang XH, Massague J. Macrophage binding to receptor VCAM-1 transmits survival signals in breast cancer cells that invade the lungs. *Cancer Cell.* 2011;20(4):538-549.

50. Erler JT, Bennewith KL, Cox TR, et al. Hypoxia-induced lysyl oxidase is a critical mediator of bone marrow cell recruitment to form the pre-metastatic niche. *Cancer Cell.* 2009;15(1):35-44.